Article

Journal of Histochemistry & Cytochemistry 2020, Vol. 68(4) 279–294

DOI: 10.1369/0022155420911930
journals.sagepub.com/home/jhc
SAGE

High-fat Diet Alters the Glycosylation Patterns of Duodenal Mucins in a Murine Model

Maria Mastrodonato, Giuseppe Calamita, Donatella Mentino, and Giovanni Scillitani
Department of Biology (MM, DM, GS) and Department of Biosciences, Biotechnology and Biopharmaceutics (GC), University of Bari "Aldo Moro," Bari, Italy.

Summary
High-fat diet (HFD) alters the glycosylation patterns of intestinal mucins leading to several health problems. We studied by histochemical and lectin-binding methods mucin alterations in the duodenum of mice fed a HFD for 25 weeks. Histochemical methods included periodic acid–Schiff, alcian blue pH 2.5, and high-iron diamine. Lectin-binding experiments were performed with SBA, PNA, WGA, MAA-II, SNA, ConA, UEA-I, LTA, and AAA. SBA, PNA, WGA, MAA-II, and SNA were tested also after desulfation and ConA after periodate-sodium borohydrate treatments (paradoxical ConA). Duodenal mucins are secreted by Brunner's glands and goblet cells in the villi. Brunner's glands of HFD mice showed increased secreting activity and a general reduction of glycosylated residuals, such as fucose and terminal α1,4-linked GlcNAc. Moreover, a general reduction of glycosylated residuals in the goblet cells of villi such as the fucosylated and sulfated ones was observed. Since the cited residuals are involved in cytoprotective and cytostatic functions, as well as in interactions with the intestinal microbiota and protection against parasites and inflammatory disorders, we conclude that HFD can predispose duodenum to several possible health disorders. (J Histochem Cytochem 68:279–294, 2020)

Keywords
glycosylation, gut microbiota, high-fat diet, mouse model, mucins

Introduction

The luminal surface of the intestinal tract is covered with glycan structures, forming both the glycocalyx of the epithelial cells and the outer secreted mucus layer.[1] Most of them are in form of mucins, that is, heavily glycosylated proteins with the capability of retaining water and forming gels. The major intestinal secreted mucin is expressed by *MUC2* in humans and by its homologous *Muc2* in rodents.[2] This mucin presents several O-linked saccharidic chains, often sialylated and/or sulfated. The chains are attached to the central part of the backbone protein. In this region, two PTS domains are found, rich in proline, serine, or threonine.[3] Intestinal mucins are involved in several functions, such as protection, lubrication, modulation of absorption, interactions with the microbiota, immunoregulation, coordination of cell proliferation, differentiation, and apoptosis.[1,3–5] In the colon, the secreted mucus barrier forms two layers, that is, an outer one colonized by the microbiota and an inner one adherent to the epithelium acting as a barrier against microorganisms.[2] In the small intestine, there is only a single layer and its function is still poorly understood, being probably involved in trapping antibiotic substances secreted by the epithelium to contrast bacteria penetration.[6]

Mucin amount and composition are known to vary to adapt to physiological and pathological conditions.[2,6–10] Altered glycosylation is in turn linked to inflammatory disease states, cancer/tumorigenesis, and increase of susceptibility to pathogens,[10–12] so that the detection

Received for publication December 6, 2019; accepted February 18, 2020.

Corresponding Author:
Maria Mastrodonato, Department of Biology, University of Bari "Aldo Moro," via Orabona 4a, 70125 Bari, Italy.
E-mail: maria.mastrodonato@uniba.it

Journal of Histochemistry & Cytochemistry

of altered glycans has been proposed as a tool in early diagnosis, disease monitoring, and prognosis.[13–15] Diet can alter the intestinal glycome as well,[16] as in the case of high-fat diet (HFD), typical to Western-style eating habits. This is one of the most studied diets, predisposing to health problems, such as obesity, insulin resistance, type 2 diabetes, dyslipidemia, steatosis, and steatohepatitis.[17–19] Alteration of gut microbiota and intestinal glycosylation have also been observed consequent to HFD.[20,21] In rats, HFD in dams can even affect intestine glycosylation in suckling pups, resulting in a decrease of fucosylation in the brush border of enterocytes.[22] HFD does not affect the glycan composition of the brush border of adult mice,[23] whereas an increase in the sialo/sulfomucins ratio and an over-expression of both Galβ1,3GalNAc and GalNAc terminal residues was observed in the colonic mucins.[21] In the duodenum, loss of O-glycans in Double Knockout mice predispose to spontaneous tumorigenesis,[6] whereas HFD promotes tumor progression with oncogenic Kras mutations and down-regulation of mucin synthesis.[24]

Apart from *Muc2* mucins produced by the goblet cells, the secreted mucus also contains mucins from the Brunner's glands. These are encoded by the *MUC6*/*Muc6* gene[25] and differ from the *MUC2*/*Muc2* in lacking acidic residuals and having more complex patterns of glycosylation.[26–28] Besides, *MUC6*/*Muc6* is rich in terminal α1,4-linked GlcNAc, which acts both as natural antibiotic and as tumor suppressor for differentiated-type adenocarcinoma.[29] Similar to *MUC2*/*Muc2*, glycosylation of *MUC6*/*Muc6* can be altered by diet or pathological conditions.[30,31]

Following our previous study with mice on the effects of HFD on the glycosylation of colonic mucins,[21] in the present work we use a histochemical approach to investigate the effects of the fat diet on the mucins secreted by the duodenum. In particular, we evaluate whether HFD alters the glycosylation of *Muc6* and *Muc2* mucin as seen for colonic *Muc2*.

Materials and Methods

Animals

Four-week-old C57BL/6J male mice were purchased from Charles River, Calco, Italy. All mice were housed in air-conditioned room with 12/12 hr dark-light cycle and allowed free access to diet and water ad libitum. To evaluate the effect of HFD on the composition of the duodenal mucins, samples of duodenal mucosa were obtained from 12 mice subdivided into two groups (n=6 in each group): control group (CTRL) were fed a standard chow diet consisting of 4% fat, 19% proteins, 6% fibers, and 12% water (10% calories from fat), and HFD group (HFD) receiving a diet composed of 42% fat, 21.6% proteins, 3% fibers, and 4% water (55% calories from fat). Both diets were purchased from Altromin-Rieper (Vandoies, Italy). The body mass was measured, and all the animals were killed by cervical dislocation (following an overnight fasting) after 25 weeks of diet. Subsequently, duodenum and liver were rapidly removed. Liver samples were used as reference to ascertain the effects of HFD by evaluating weight of the whole organ and lipid storage in hepatocytes while the samples of duodenum were processed for histochemistry. All the studies were approved by the animal care and use Committee of the University of Bari (OPBA di Ateneo) and the Italian Ministry of Health (authorization n. 326/2018-PR).

Section Preparation

Two duodenal samples were collected from each animal, and immediately fixed in 10% neutral buffered formalin, dehydrated in a graded series of ethanol and then embedded in paraffin wax as detailed elsewhere.[32] Sections were serially cut at 5 μm.

Liver samples were fixed in 4% glutaraldehyde in TBS 0.1 M, pH 7.4, and after an overnight wash in the same buffer, were post-fixed with 1% osmium tetroxide in TBS for 2 hr at 4C. Osmium tetroxide also stained in gray lipid droplets. Fixed specimens were processed for embedding in Epoxy Resin-Araldite (M) CY212 (TAAB, Aldermaston, England) as previously reported.[33] Semithin sections were serially cut into 2-μm-thick sections and observed without staining to assess lipid droplet stores and the extent of steatosis.

Classic Histochemical Staining

Samples of duodenum were stained with periodic acid-Schiff (PAS), alcian blue (AB) at pH 2.5, and high-iron diamine (HID) to demonstrate carbohydrates with 1,2 glycols, acidic residuals (both sialylated and sulfated), and sulfated residuals, respectively. Counterstaining with Mayer's hematoxylin (HE) was performed. Protocol details were given elsewhere.[34] All the reactives cited in this section were from Sigma-Aldrich (St. Louis, MO).

Fluorescent Lectin Binding

A panel of 9 FITC-labeled lectins (SBA, PNA, MAA-II, SNA, WGA, ConA, UEA-I, LTA, and AAA) was selected among the most commonly used to detect the main residuals in the oligosaccharidic chains of mucins.

Table 1. Lectins Used and Their Carbohydrate Specificities.

Lectin	Source	Binding Specificity	Lectin Concentration (mg/ml)	Inhibitory Sugar
SBA	*Glycine max*	GalNAc/Gal	0.02	0.2 M GalNAc
PNA	*Arachis hypogaea*	Galβ1,3GalNAc	0.06	0.2 M Gal
WGA	*Triticum vulgaris*	(GlcNAcβ1,4)n	0.02	0.01 M TACT
MAA-II	*Maackia amurensis*	Neu5Acα2,3Galβ1,3GalNAc	0.02	0.02 M Neu5Ac
SNA	*Sambucus nigra*	Neu5Acα2,6Gal/GalNAc	0.02	0.2 M Neu5Ac
ConA	*Canavalia ensiformis*	D-Man, D-Glc	0.05	0.1 M MαM
UEA-I	*Ulex europaeus*	Fucα1,2	0.10	0.2 M L-Fuc
LTA	*Tetragonolobus purpureus*	L-Fucα1,6GlcNAc L-Fucα1,2Galβ1,4 [L-Fuc1,3] GlcNAcβ1,6R	0.10	0.2 M L-Fuc
AAA	*Aleuria aurantia*	Fucα1,6GlcNAcβNAsn Fucα1,3, Fucα1,4	0.10	0.2 M L-Fuc

Abbreviations: GalNac, N-acetylgalactosamine; Gal, galactose; GlcNac, N-acetylglucosamine; TACT, N, N,' N"-triacetylchitotriose; Neu5Ac, N-acetylneuraminic acid; Man, mannose; Glc, glucose; MαM, methyl-α-mannopyranoside; Fuc, fucose.

Details for the lectins employed, their concentrations, their sugar specificities, and the abbreviations used for glucidic residues are summarized in Table 1. All lectins were from Vector Laboratories (Burlingame, CA). Lectin protocols followed dealer's indications with minor modifications reported elsewhere.[35] Sections of duodenum underwent incubation for 1 hr at room temperature with the lectin solution in HEPES. After rinsing in the same buffer, they were mounted in Fluoromount for observation. Controls for lectin labeling included (1) substitution of each lectin with HEPES alone, (2) incubation with lectin added to an inhibitory sugar (types and concentrations given in Table 1, and (3) binding to samples from other sources presenting mucins that were previously demonstrated to be labeled by lectins tested in this paper, that is, the secreting epithelia of colon of mouse and the egg extra-cellular matrix of the toad *Bufo bufo*.[36,37] The binding of WGA, SBA, and PNA lectins was also tested with a desulfation pre-treatment by a sequence of methylation-saponification.[29] Stable class-III mucins[38] were detected by the paradoxical ConA binding staining (PCS), consisting in a sequence of 1% periodate and 0.2% sodium borohydrate in 1% sodium biphosphate treatments before ConA labeling.[39] Except for lectins, all the reactives cited in this section were from Sigma-Aldrich.

Image Processing for Classic Histochemical Staining

Photographic documentation was shot in bright light by an Eclipse E600 photomicroscope equipped with a DMX1200 digital camera (Nikon Instruments SpA, Calenzano, Italy) under the same conditions for all the stains, tracts, and samples. One to three photos per individual were taken at 400x with a resolution of 150 dpi.

Brunner's glands sizes were compared between CTRL and HFD groups by recording the transverse diameters of both glands and related lumina chosen among those having the best orientation. Ten glands per individual were selected, for a total of 60 glands per group.

An analysis of the variation of the intensity of each stain between CTRL and HFD groups was performed for both Brunner's glands and duodenal goblet cells. For Brunner's glandular cells, up to five sample areas of 900 μm^2 in each photo were selected. For the goblet cells, 10 cells with the best orientation were selected in each photo. The staining intensities were estimated by computing integrated optical density (OD) values from RGB photographs processed by the color deconvolution method.[40] Color channels relative to the stain, the counterstain, and the background were separated. Stain vectors were created from single-stain slides without counterstaining.[41] Single cell ODs were then computed from mean intensities in each stain channel.[42] Staining of the enterocyte glycocalyx was also recorded, but its intensity was not measured. Analyses were performed by the Image J package[43] implemented with the color deconvolution plugin.[41]

Image Processing for Fluorescent Lectin Binding

Photographic documentation was shot in epifluorescence under 495 nm light by the same photomicroscope device as previous with sensibility set to 4.' An analysis of the variation of the intensity of each lectin-binding between CTRL and HFD groups was performed for both Brunner's glands and duodenal goblet cells. One to three photos per individual were taken at 200x with a resolution of 150 dpi. For the image analysis of Brunner's glands, up to five sample areas of 2500 μm^2 in each

photo were selected. For the analysis of goblet cells, 10 cells with the best orientation were selected in each photo. The lectin-binding intensities were estimated by computing for each area or cell the corrected total cell fluorescence (CTFC).[44] In order to avoid computing and representing too large CTFC values, all data were divided by 10^7. Analyses were performed by the Image J package.[43] Additionally, lectin binding to the enterocyte glycocalyx was recorded, but its intensity was not evaluated because it was difficult to measure such a relatively thin and somewhat discontinuous structure with our methods.

Statistical Analysis

For the comparison of Brunner's glands size between CTRL and HFD, the most common descriptive statistics (mean, standard deviation, median, kurtosis, and skewness) were computed from both glands and lumina transverse diameters.[45] Significant deviation from normality of distribution of data was estimated by Shapiro-Wilk tests from skewness and kurtosis values. Significant variation of the cited measures between CTRL and HFD groups was estimated by both parametric Student's t-test and non-parametric Mann-Whitney's U test.

For the analysis of the variation of the intensity of each histochemical stain or lectin-binding between CTRL and HFD groups in both Brunner's glands and duodenal goblet cells, mean OD or CTFC values were compared between CTRL and HFD by both Student's t-test and Mann-Whitney's U tests as previous. Statistical computations for the aforementioned analyses were generated by an Excel plugin, the Real Statistics Resource Pack software (Release 6.2).[46]

Results

Classic Histochemical Staining

Liver. The liver of CTRL mice presented hepatocytes with few lipid microvesicles (Fig. 1A), whereas in the HFD group, it showed hepatocytes with several micro- and macrovesicles, indicating severe steatosis (Fig. 1B).

Brunner's Glands. The transverse diameters of Brunner's glands did not differ between CTRL and HFD, whereas the diameters of the lumina were significantly higher in the latter (Fig. 2A and B), as indicated by the statistical tests (resumed in Table 2). Brunner's gland cells were intensely and uniformly positive to PAS (Fig. 2A), whereas in HFD, the stain was weaker and concentrated in the subapical area of cells (Fig. 2B). OD values of PAS in HFD resulted significantly lower than CTRL with both Student's t and Mann-Whitney's U tests (Table 3). Brunner's glands resulted always negative for both AB pH 2.5 and HID stains (Fig. 2C to F).

Villar Goblet Cells. PAS and AB pH 2.5 stained intensely the goblet cells in both the CTRL and HFD (Fig. 2G to J) with no significant difference of ODs between groups (Table 3). On the contrary, a significant decrease was observed for HID stain in the HFD in respect to the CTRL (Fig. 2K and L; Table 3). The glycocalyx of enterocytes resulted positive to all stains in both CTRL and HFD (Fig. 2G to L), but its intensity was not measured. Statistical comparisons of ODs in Brunner's and villar secreting cells are resumed in the histogram of Fig. 3.

Fluorescent Lectin Binding

Brunner's Glands. SNA and MAA-II lectins did not bind to the secretory cells. In general, binding intensity as measured by CTFC was significantly higher in CTRL than in HFD groups (Fig. 4). PNA binding was mostly observed in the deeper part of the adenomeres. A neat decrease of binding intensity in HFD was observed with PCS (Fig. 4I and J). Statistical analyses for lectin-binding intensity are reported in Table 4 and resumed in the histogram of Fig. 5.

Villar Goblet Cells. LTA, SNA, and PCS binding were never observed. MAA-II binding resulted only in the crypts (Fig. 6M and N). Desulfation resulted in an increase of SBA, PNA, WGA, and MAA-II binding only in CTRL (Fig. 6A to P). After desulfation, few cells in the crypts bound also to SNA, but they were not considered in the analyses. Significant differences between CTRL and HFD resulted for all the lectins, with higher CTFC values observed in CTRL than in HFD (Figs. 6 and 7). Statistical analyses for lectin-binding intensity are reported in Table 5 and resumed in the histogram of Fig. 8.

The glycocalyx of enterocytes bound to SBA, PNA, WGA, ConA, UEA, and AAA (Figs. 6 and 7), and no differences were observed between groups.

Discussion

Proximal duodenum mucins are secreted by the cells of the Brunner's glands and the goblet cells in the villi. Similar to the colon, the main mucin is expressed by *MUC2*/*Muc2*, which forms a viscoelastic gel lining the lumen, but its structural arrangement and

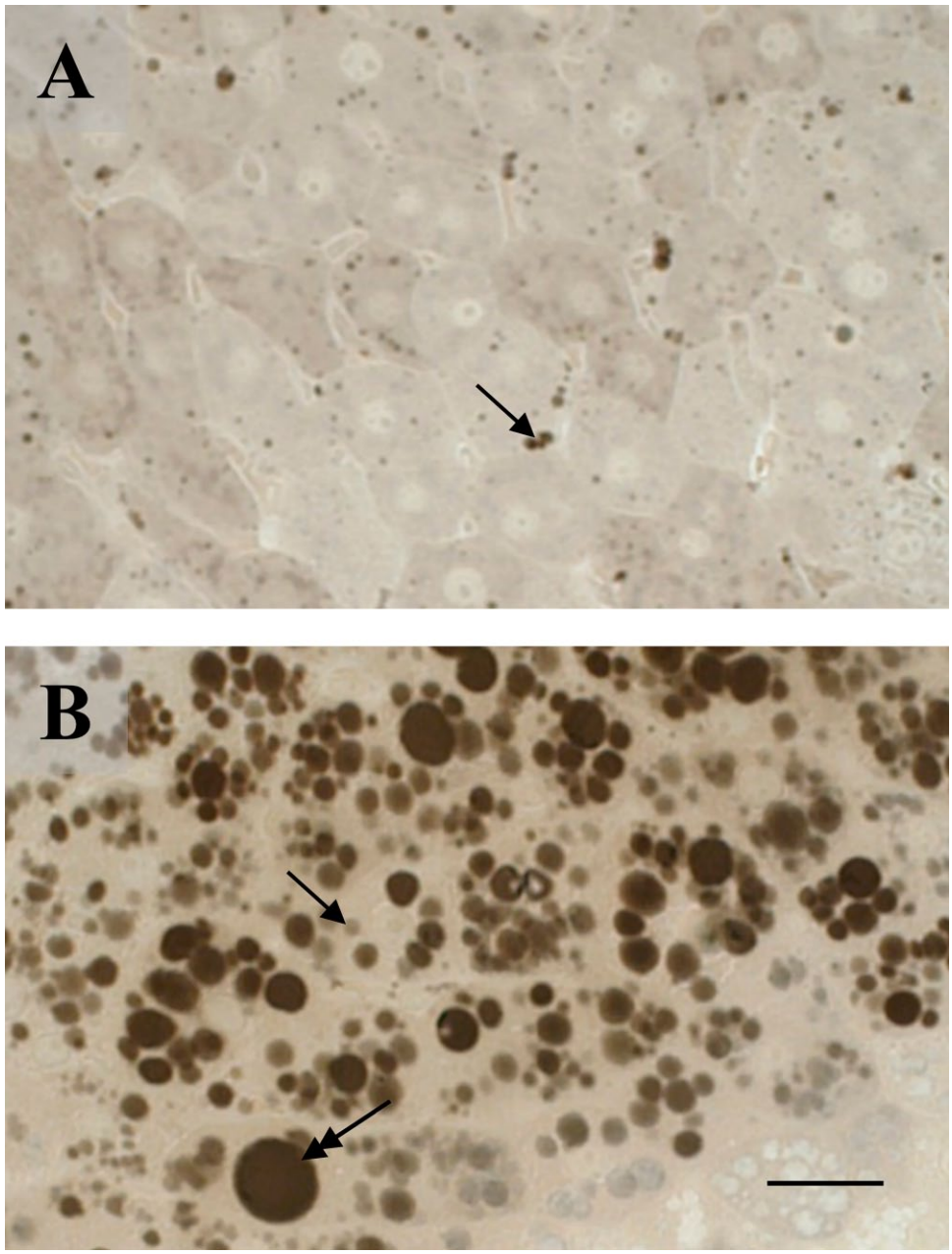

Figure 1. Fat accumulation in the livers of control and high-fat diet (HFD) fed mice. Few microvesicles (arrow) are seen in the control liver (A) whereas the HFD liver (B) shows a number of microvesicles (arrow) together with macrovesicles (double headed arrow). (A, B) Osmium tetroxide post-fixation. Scale bar=25 μm.

functions are different. In the duodenum, mucus polymers form a single, non-adherent layer,[47] whereas in the colon there are two layers of mucus, the inner one adhering to the epithelium where it forms a physical barrier to bacteria and the outer one hosting a dense microbiota. Rather than a barrier, the mucus layer in the duodenum is thought to form a gradient of antibacterial substances secreted by the epithelial cell decreasing the diffusion rate of bacteria.[1,3,4] The differences between colon and duodenum mucins are due to different glycosylation patterns[3,47] that can be altered in pathological processes like those arising from HFD.[20–25] The analysis of mucin glycopatterns by histochemical, lectin-binding, and immunohistochemical methods provides a useful tool in the detection of the above reported

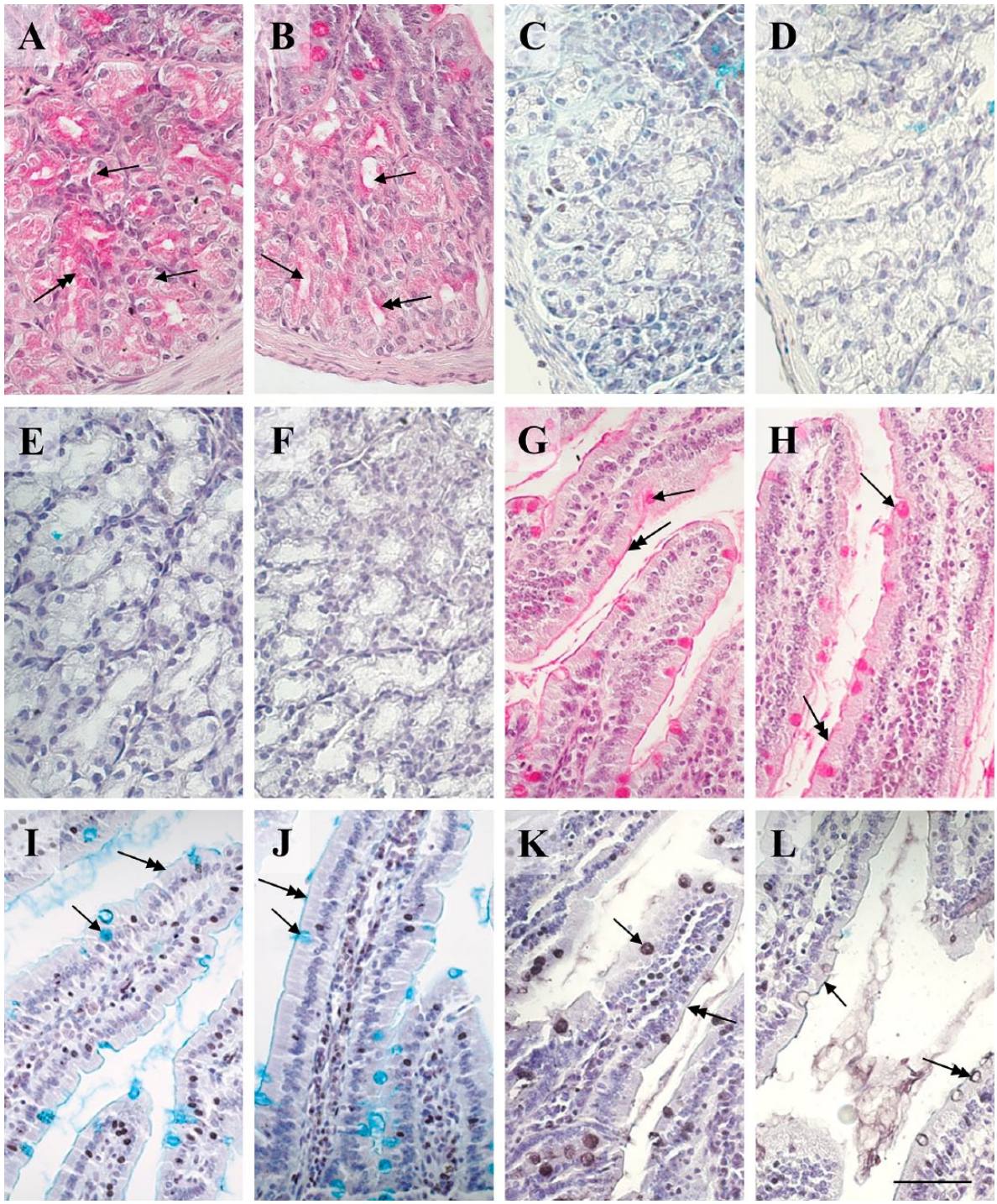

Figure 2. Histochemistry of Brunner's glands and villi of control and HFD mice. (A) Brunner's glands in the control specimen show smaller lumina (arrows) and secretion (double headed arrow) is intensely stained by PAS for carbohydrates and distributed rather uniformly. (B) In respect to control, Brunner's glands in the HFD condition present larger lumina (arrows) and the PAS-positivity of the secretion is weaker (double headed arrow), concentrated in the subapical area of cells. (C–F) Brunner's glands in both control (C, E) and HFD (D, F) are negative to AB pH 2.5 (C, D) and HID (E, F) stains for acidic residuals. (G, H) Villi present goblet cells (arrows) and glycocalyx (double headed arrows) positive to PAS stain without difference of intensity between control (G) and HFD (H). (I, J) Villi present goblet cells (arrows) and glycocalyx (double headed arrows) positive to AB pH 2.5 stain for acidic residuals with no apparent difference of intensity between control (I) and HFD (J). (K, L) Villi present goblet cells (arrows) and glycocalyx (double headed arrows) positive to HID stain for sulfated glycans that is more intense in control (K) than in HFD (L). (A, B, G, H) PAS-hematoxylin. (C, D, I, J) Alcian blue pH 2.5-hematoxylin. (E, F, K, L) HID-hematoxylin. Scale bar=50 μm. Abbreviations: HFD, high-fat diet; PAS, periodic acid-Schiff; HID, high iron diamine; AB, alcian blue.

Table 2. Statistical Comparisons of Diameters (in µm) of Brunner's Glands and Related Lumina Between Controls (CTRL) and High-fat Diet (HFD) Fed Groups.

	n	Mean (±SD)	Median	Range	Rank Sum	W-stat	*t*-test (*df*)	U
Gland diameter								
CTRL	60	25.810 (3.734)	25.387	16.978	3303	0.969		
HFD	60	27.125 (5.254)	27.332	22.532	3957	0.973	1.581 (118)	1473
Lumen diameter								
CTRL	60	8.987 (3.539)	9.662	18.942	3145	0.983		
HFD	60	10.778 (3.343)	11.044	13.522	4115	0.979	2.850* (118)	1315*

Abbreviations: *N*, sample size; SD, standard deviation; W-stat, Shapiro-Wilk test for normality of distribution computed from skewness and kurtosis; t-test, value of Student's t-test; *df*, degrees of freedom for statistical tests; U, value of Mann-Whitney's U test. *Probability value associated to the test significant for $p<0.05$.

Table 3. Statistical Comparisons of OD Values From Histochemical Analyses of Brunner's Glands and Villar Goblet Cells Between Controls (CTRL) and High-fat Diet (HFD) Fed Groups.

OD	*N*	Mean (±SD)	Median	Range	Rank Sum	W-stat	*t*-test (*df*)	U
PAS Brunner								
CTRL	119	2.139 (0.255)	2.152	1.147	20,517	0.983		
HFD	122	1.644 (0.198)	1.622	0.987	8403	0.988	16.741* (238)	1022*
PAS Villi								
CTRL	123	1.775 (0.376)	1.764	1.879	15,404	0.993		
HFD	121	1.730 (0.267)	1.750	1.541	13,999	0.990	1.224 (240)	6618
AB pH 2.5 Villi								
CTRL	120	2.001 (0.304)	1.993	1.399	14,898	0.991		
HFD	124	1.989 (0.380)	2.032	2.100	14,748	0.995	0.354 (241)	7245
HID Villi								
CTRL	121	2.875 (0.323)	2.866	1.935	22,054	0.986		
HFD	120	2.045 (0.266)	2.022	1.334	7836	0.990	21.925* (242)	333*

Abbreviations: OD, optical density; *N*, sample size; SD, standard deviation; W-stat, Shapiro-Wilk test for normality of distribution computed from skewness and kurtosis; *t*-test, value of Student's t-test; *df*, degrees of freedom for statistical tests; U, value of Mann-Whitney's U test; PAS, periodic acid-Schiff; AB, alcian blue; HID, high iron diamine. *Probability value associated to the test significant for $p<0.05$.

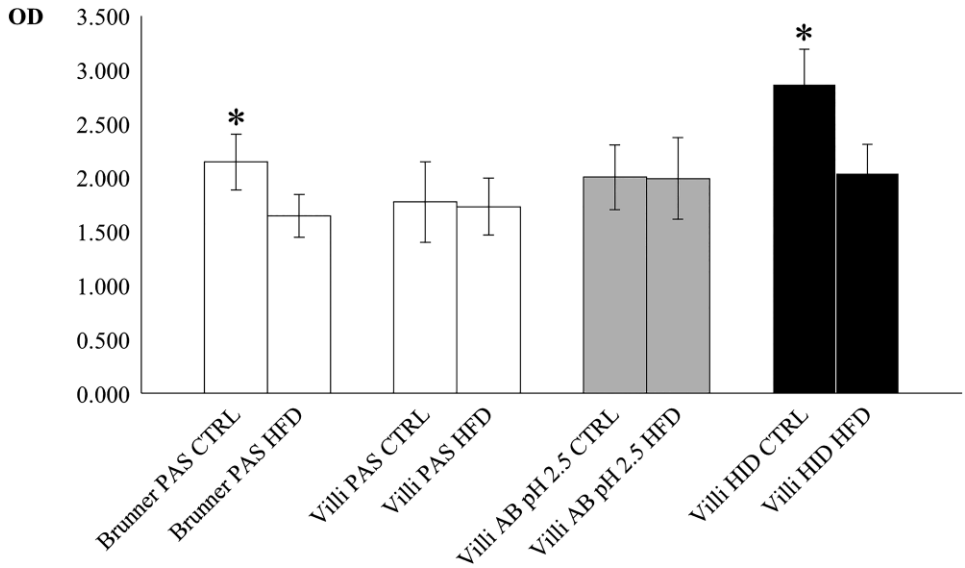

Figure 3. Plot of mean (±SD) optical density (OD) for the histochemical stains PAS (white), alcian blue pH 2.5 (gray), and HID (black) of Brunner's glands and villar goblet cells in control (CTRL) and high-fat diet (HFD) fed mice. Asterisks indicate statistically significant differences of control mean values in respect to corresponding HFD (see text for details). Abbreviations: SD, standard deviation; PAS, periodic acid-Schiff; HID, high iron diamine; AB, alcian blue.

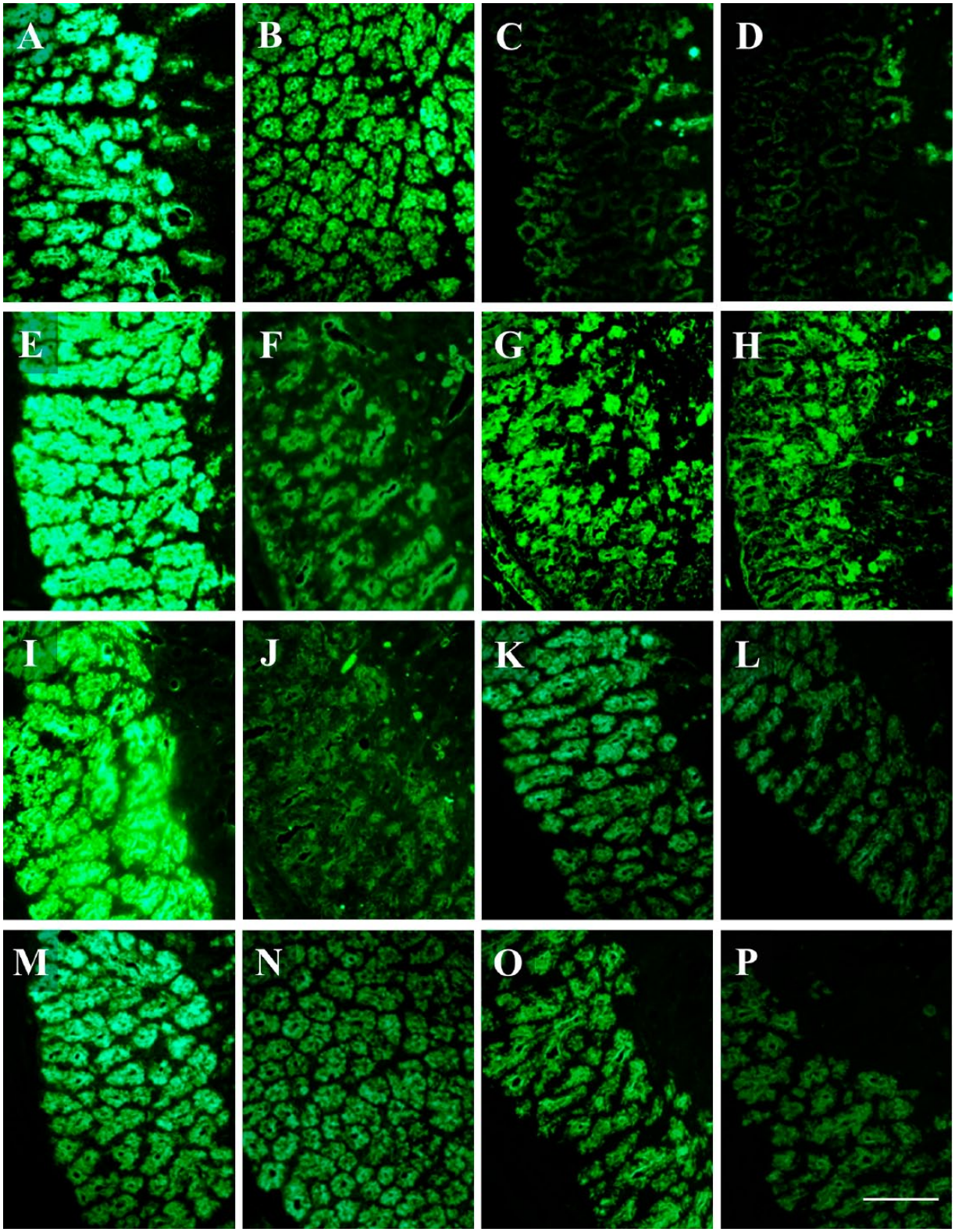

Figure 4. Lectin-binding of Brunner's glands of control and high-fat diet fed mice. The intensity of binding in secreting cells is higher in the control (A, E, G, I, K, M, O) than in the HFD (B, F, H, J, L, N, P) specimen, except for PNA (C, D). (A, B) SBA-FITC. (C, D) PNA-FITC. (E, F) WGA-FITC. (G, H) ConA-FITC. (I, J) Paradoxical-ConA-FITC. (K, L) UEA-I-FITC. (M, N) AAA-FITC. (O, P) LTA-FITC. Scale bar=50 μm. Abbreviation: HFD, high-fat diet.

Table 4. Statistical Comparisons of CTFC Values From Histochemical Analyses of Brunner's Glands Between Controls (CTRL) and High-fat Diet (HFD) Fed Groups.

Lectin	*N*	Mean (±SD)[a]	Median[a]	Range[a]	Rank Sum	W-stat	*t*-test (*df*)	U
SBA								
CTRL	118	107.578 (8.956)	107.994	49.046	21,369	0.985		
HFD	122	65.915 (13.147)	65.282	56.288	7551	0.983	28.599* (238)	48*
PNA								
CTRL	120	6.973 (2.749)	6.928	14.781	13,924	0.983		
HFD	120	7.112 (1.372)	7.220	6.858	14,996	0.990	0.495 (238)	6664
WGA								
CTRL	122	96.036 (11.995)	95.672	62.308	17,982	0.990		
HFD	119	86.143 (12.120)	86.391	69.803	11,179	0.995	6.369* (239)	4039*
ConA								
CTRL	121	110.404 (4.077)	110.543	25.441	21,512	0.984		
HFD	120	91.318 (8.334)	90.957	48.073	7649	0.988	22.612* (239)	389*
PCS								
CTRL	118	106.633 (8.282)	106.741	50.730	21,299	0.976		
HFD	121	39.143 (11.734)	39.682	49.545	7381	0.983	51.258* (237)	0*
UEA-I								
CTRL	119	37.249 (8.582)	37.578	40.931	19,789	0.994		
HFD	121	24.978 (5.703)	24.615	31.731	9,131	0.980	13.066* (238)	1750*
LTA								
CTRL	122	29.514 (3.669)	29.375	29.354	22,022	0.904*		
HFD	121	17.336 (4.466)	17.929	23.483	7624	0.988	23.235 (241)	243
AAA								
CTRL	122	58.098 (9.211)	58.918	47.385	22,167	0.994		
HFD	122	31.649 (7.939)	31.676	44.138	7723	0.991	24.024* (242)	220*

Abbreviations: CTFC, corrected total cell fluorescence; *N*, sample size; SD, standard deviation; W-stat, Shapiro-Wilk test for normality of distribution computed from skewness and kurtosis; t-test, value of Student's t-test; *df*, degrees of freedom for statistical tests; U, value of Mann-Whitney's U test.
*Probability value associated to the test significant for $p<0.05$.
[a]Real values are x 107.

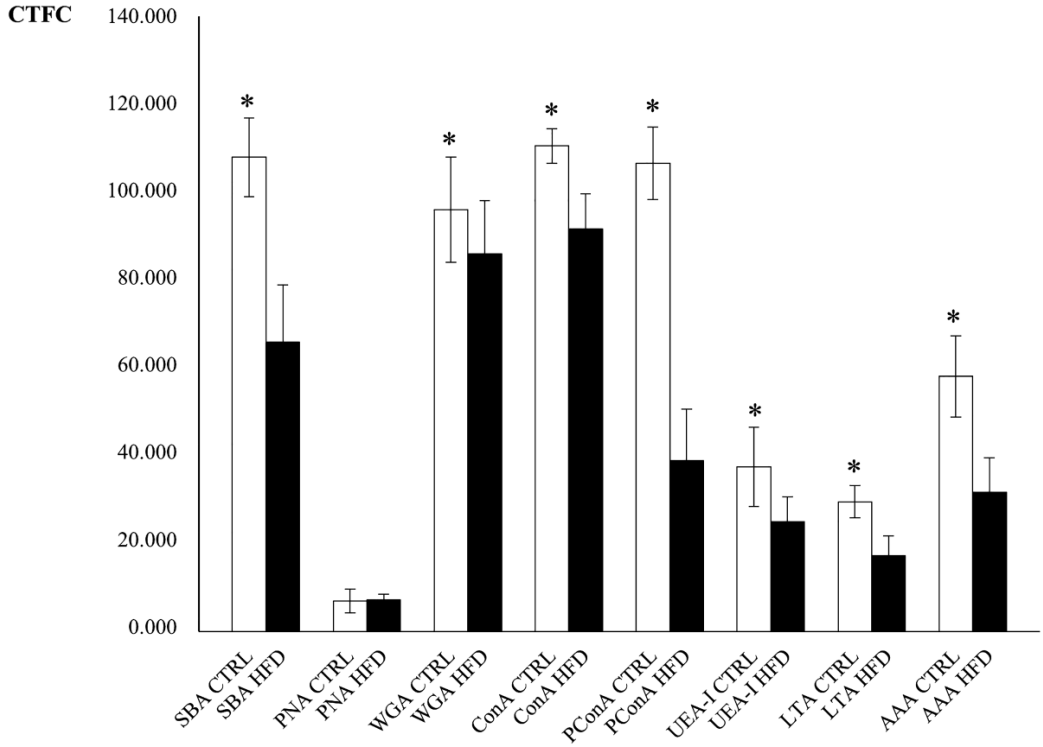

Figure 5. Plot of mean (±SD) corrected total cell fluorescence (CTFC) values for lectin-binding of Brunner's glands in control (CTRL, white) and high-fat diet (HFD, black) fed mice. Asterisks indicate statistically significant differences of control mean values in respect to corresponding HFD (see text for details). Abbreviations: SD, standard deviation; HFD, high-fat diet; PConA, paradoxical ConA.

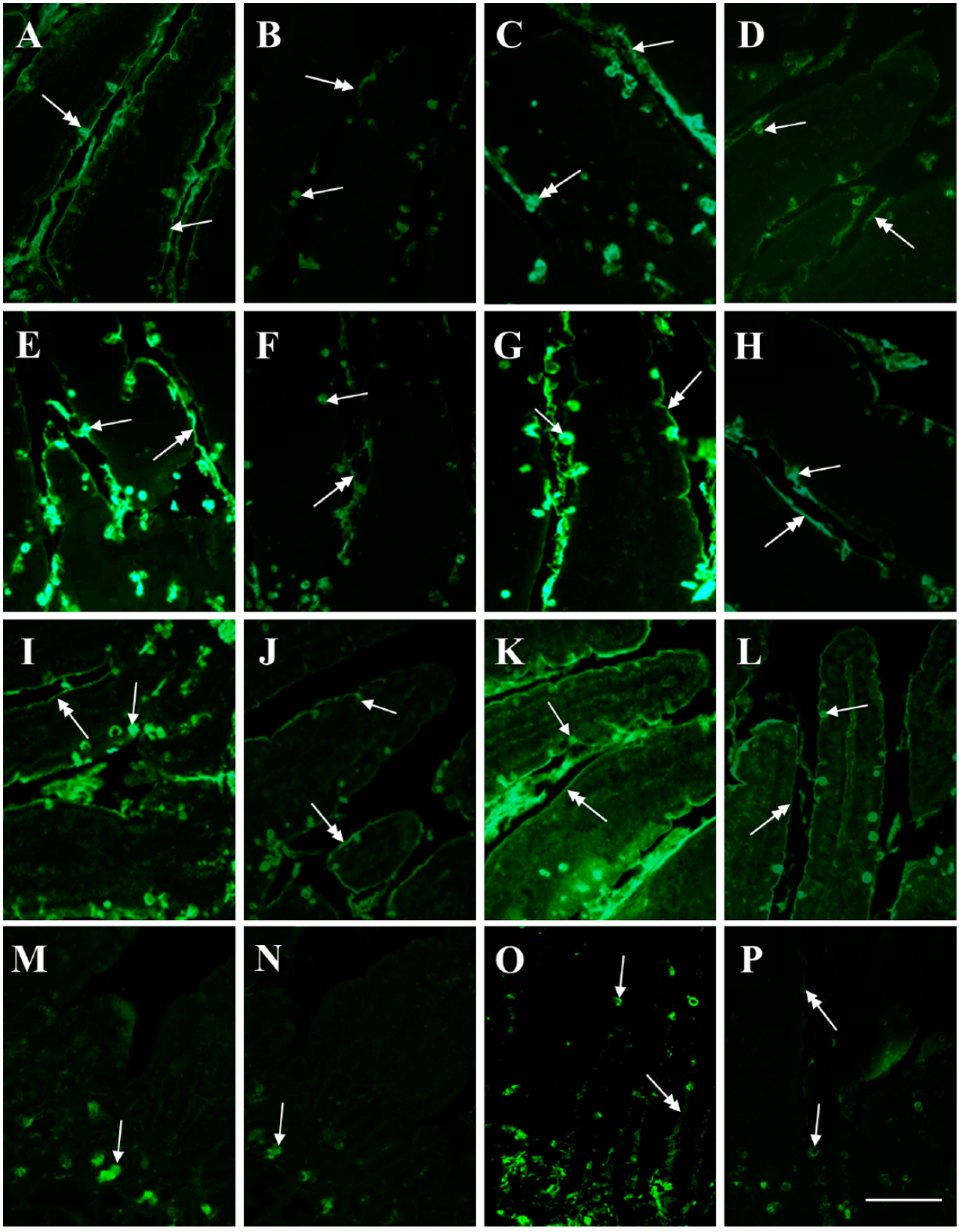

Figure 6. Lectin-binding of goblet cells (arrows) and glycocalyx (double headed arrows) of villi in control and high-fat diet (HFD) fed mice. The intensity of binding in goblet cells is higher in the control (A, E, I, M) than in the HFD (B, F, J, N) specimen. After desulfation, lectin-binding increases in control (C, G, K, O) but not in HFD (D, H, L, P). (A, B) SBA-FITC. (C, D) desulfation SBA-FITC. (E, F) PNA-FITC. (G, H) desulfation PNA-FITC. (I, J) WGA-FITC. (K, L) desulfation WGA-FITC. (M, N) MAA-II-FITC. (O, P) desulfation MAA-II-FITC. Scale bar=50 μm.

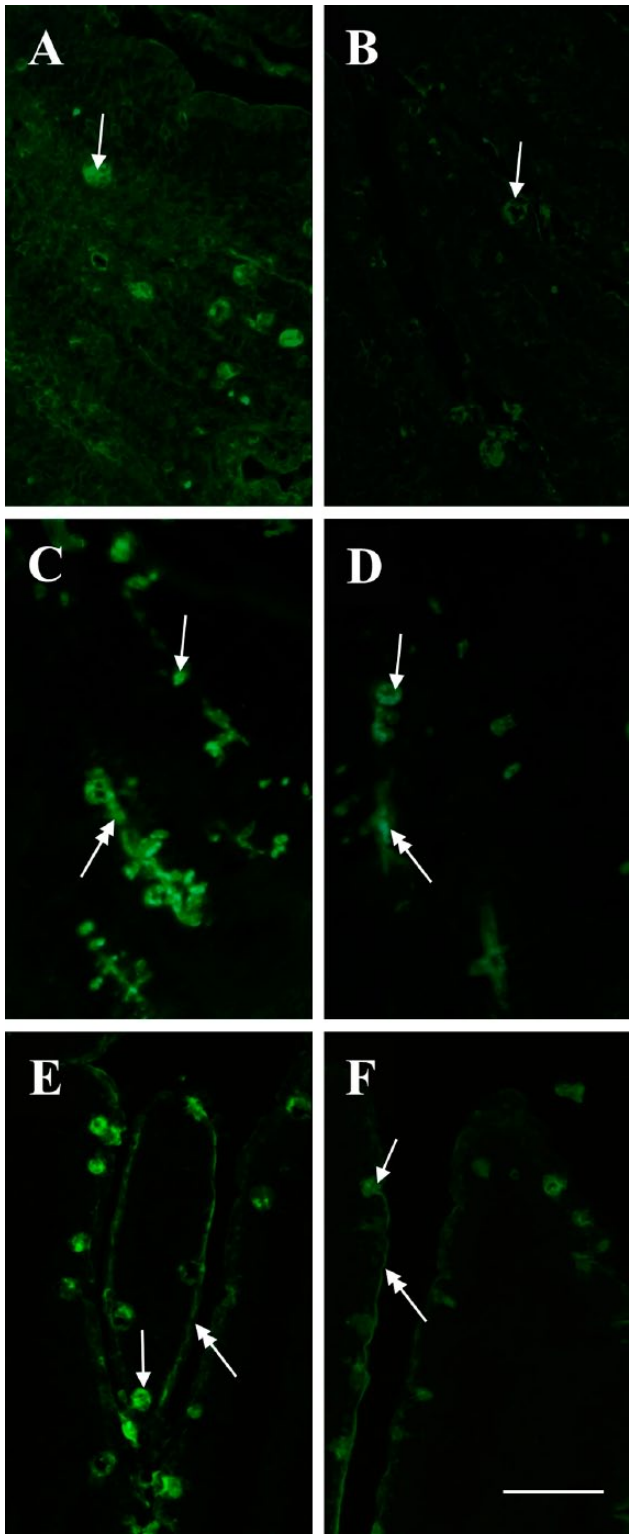

Figure 7. Lectin-binding of goblet cells (arrows) and glycocalyx (double headed arrows) of villi in control and HFD mice. The intensity of binding in goblet cells is higher in the control (A, C, E) than in the HFD (B, D, F) specimen. (A, B) ConA-FITC. (C, D) UEA-I-FITC. E, F AAA-FITC. Scale bar=50 μm. Abbreviation: HFD, high-fat diet.

oligosaccharide alterations.[13–15] In the present work, we show that HFD alters the glycosylation pattern of duodenum mucins in a way similar to that we previously found in the colon.[21]

It should be noted that often the link between stain intensity and amount of reaction products is not linear as it should be according to the Lambert-Beer law,[41] but it is still useful in comparative analyses like those presented here. In image analysis, usually homogenous areas are selected for the evaluation of the stain intensity, like we did with the Brunner's glands, but this approach was not possible with the goblet cells in the villar epithelium because they are irregularly arranged along the border of the villus. Consequently, we preferred to estimate the mean stain intensity of single cells. As far as the glycocalyx, it showed a rather variable thickness, so we did not measure its staining intensity but recorded only its positivity with stain or binding.

Liver steatosis, that is, abnormal accumulation of triglycerides in hepatocytes, is one of the consequences of HFD diet.[48] Having observed several steatotic hepatocytes in the HFD group, we concluded that the experimental treatment was effective.

The lumen of the Brunner's glands in the HFD was significantly larger than that of the control group, and this can be interpreted as an increase of the secretion rate.[49] This could result in a lower amount of stored mucins and explain the significant lower value of OD in respect to the control. Similar results were observed in Guinea pig's isolated glands after stimulation with hormonal, inflammatory, and neurocrine agents.[49] On the other side, mice were fastened overnight showing reduced secretion. Likely, the lower staining intensity seen in the HFD condition was due to a reduction in mucin glycosylation. Negative stain with AB pH 2.5 and HID confirms the lack of acidic mucins in murine Brunner's glands, as previously observed.[28] Lectin-binding experiments indicated that in the CTRL group the oligosaccharidic chains of mucins present residuals of Gal/GalNAc (as detected by SBA/PNA), Man/Glc (ConA), GlcNAc (WGA), and fucose linked in 1,2; 1,3; 1,4; and 1,6 (UEA-I, LTA, AAA). All the cited residues are still present in the HFD group, but lower CTFC values indicate a decrease in their number. The PConA reaction was positive in the CTRL and almost negative in the HFD group indicating a massive decrease of class III mucins and thus of terminal α1,4-linked GlcNAc.[29] In the digestive system, these mucins are expressed in glandular mucous cells in the stomach (cardiac gland cells, mucous neck cells, and pyloric gland cells), in the Brunner's gland cells, and along

Table 5. Statistical Comparisons of CTFC Values From Histochemical Analyses of Villar Goblet Cells Between Controls (CTRL) and High-fat Diet (HFD) Fed Groups.

Lectin	N	Mean (SD)[a]	Median[a]	Range[a]	Rank Sum	W-stat	*t*-test (*df*)	U
SBA								
CTRL	122	3.278 (0.565)	3.281	3.304	22,339	0.987		
HFD	122	1.210 (0.625)	1.249	2.846	7551	0.984	27.109* (242)	48*
DSBA								
CTRL	122	2.062 (0.920)	1.970	5.118	18,214	0.967		
HFD	120	1.292 (0.781)	1.298	3.681	11,189	0.988	7.012* (240)	736*
PNA								
CTRL	120	6.618 (0.850)	6.597	4.642	16,663	0.981		
HFD	121	6.127 (0.915)	6.113	4.660	12,498	0.994	4.312* (239)	5117*
DPNA								
CTRL	122	8.381 (0.895)	8.474	4.584	20,841	0.982		
HFD	119	6.772 (0.691)	6.788	3.230	8320	0.990	15.592* (239)	1180*
WGA								
CTRL	121	11.236 (0.593)	11.215	3.097	21,665	0.994		
HFD	119	9.483 (0.464)	9.452	2.549	7255	0.987	25.460* (238)	115*
DWGA								
CTRL	120	11.645 (1.069)	11.695	5.481	19,422	0.996		
HFD	122	10.091 (1.212)	10.141	5.637	9981	0.991	10.571* (240)	2478*
MAA-II								
CTRL	122	2.163 (0.447)	2.122	2.514	16,681	0.986		
HFD	122	1.971 (0.393)	2.028	2.051	13,209	0.963	3.565* (242)	5706*
DMAA-II								
CTRL	120	2.700 (0.795)	2.702	3.909	17,646	0.993		
HFD	122	2.169 (0.562)	2.128	2.651	11,757	0.990	6.013* (240)	4254*
ConA								
CTRL	120	1.631 (1.077)	1.677	5.367	16,689	0.993		
HFD	121	1.109 (0.902)	1.014	4.484	12,472	0.989	4.076* (239)	5091*
UEA-I								
CTRL	120	2.455 (0.102)	2.470	5.749	19,236	0.995		
HFD	121	1.333 (0.042)	1.350	2.161	9925	0.991	10.358* (239)	2544*
AAA								
CTRL	119	2.350 (0.711)	2.327	3.449	18,561	0.993		
HFD	121	1.703 (0.387)	1.669	2.185	10,359	0.971	8.774* (238)	2978*

Abbreviations: CTFC, corrected total cell fluorescence; *N*, sample size; SD, standard deviation; W-stat, Shapiro-Wilk test for normality of distribution computed from skewness and kurtosis; t-test, value of Student's *t*-test; *df*, degrees of freedom for statistical tests; U, value of Mann-Whitney's U test.
*Probability value associated to the test significant for $p<0.05$.
[a]Real values are x 10^7.

the biliary and pancreatic ducts.[14] α1,4-linked GlcNAc residuals are linked to serine or threonine residues of the scaffold protein expressed by *MUC6* and bind to the ConA lectin after periodate-sodium borohydrate treatment.[50] *MUC6* is expressed in Brunner's glands and in other tissues in the embryonic life around the 19th week, and it is involved in epithelia cytoprotection against several substances in both fetal and adult life.[25] Besides, α1,4-linked GlcNAc residuals have a cytostatic functions and class III mucins are expressed in gastric, pancreatic, biliary, and pulmonary adenocarcinomas, serving as a tumor suppressor.[29] It has been also observed that αGlcNAc residuals act as a natural antibiotic against *Helicobacter pylori* infection.[29] Thus, the massive reduction of class III mucins in mice fed an HFD could increase the vulnerability of the duodenum to the cited diseases. The reduction of other residuals in the HFD group could increase the susceptibility to pathologies, as well. As an example, Gal/GalNAc residuals are important in preventing amoebiasis, since they interact with *Entoameba* inhibiting adhesion to the underlying epithelium.[51] Fuc residuals are involved in mucus viscosity and in modeling the microflora composition in favor of fucose-degrading commensals.[52] Changes in the

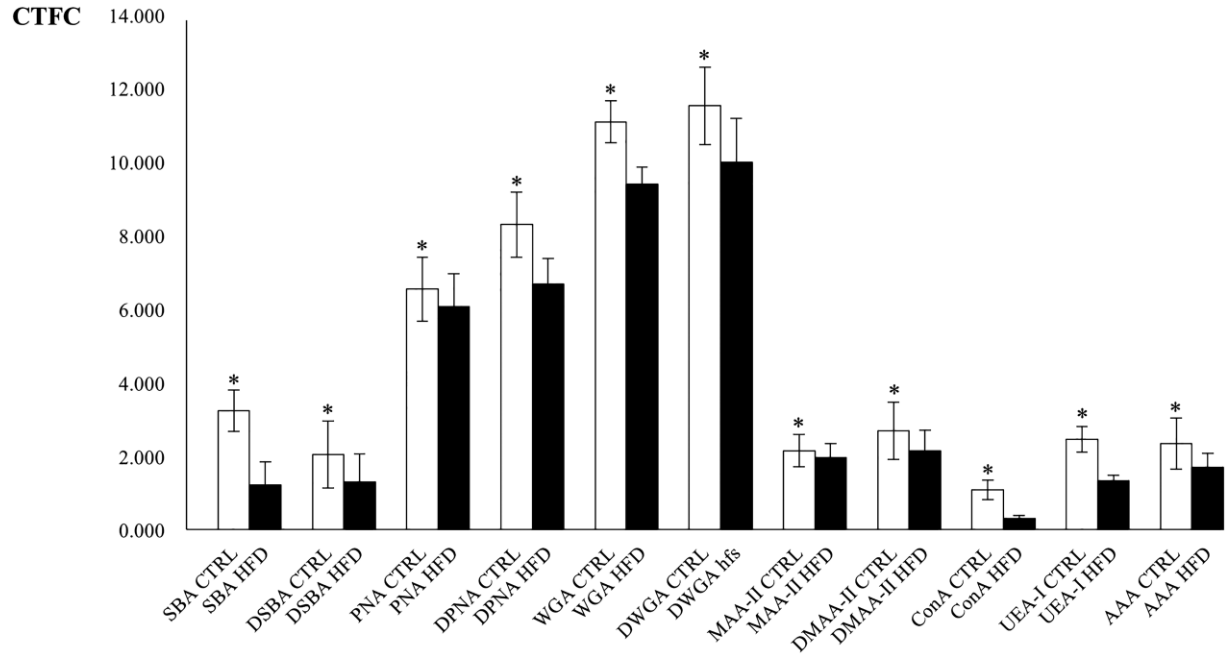

Figure 8. Plot of mean (±SD) corrected total cell fluorescence (CTFC) values for lectin-binding of villar goblet cells in control (CTRL, white) and high-fat diet (HFD, black) fed mice. Asterisks indicate statistically significant differences of control mean values in respect to corresponding HFD (see text for details). Abbreviation: SD, standard deviation.

expression of fucosylated residuals were observed in cancer and inflammation,[53] so that altered fucosylation following HFD could promote microflora alteration and pathologies.

The goblet cells of villi in the CTRL group secrete acidic mucins, as indicated by positivity to AB pH 2.5 and HID. OD values for PAS and AB pH 2.5 did not vary between CTRL and HFD groups, indicating that neutral and acidic carbohydrate amounts were not affected by the treatment. On the opposite, OD for HID stain was significantly lower in HFD, suggesting a decrease in the sulfation of glycans. This finding parallels the condition of mucins in the mouse colon, in which desulfation was observed in HFD-fed individuals.[21] Sulfated residuals are involved in regulating the interactions with microorganisms and parasitic helminths, as well as in preventing inflammatory disorders.[1,11,54] Thus, it is reasonable to hypothesize that the reduction of sulfation in duodenal glycans leads to pathophysiological alterations.

Lectin-binding experiments in the CTRL group showed the presence of residuals of Gal/GalNAc (SBA/PNA), GlcNAc/NeuNAc (WGA, MAA-II), Man/Glc (ConA), and fucose linked in 1,2; 1,3; 1,4; and 1,6 (UEA-I, AAA). Desulfation experiments resulted in an increase of binding for SBA, PNA, WGA, and MAA-II, suggesting that sulfated residuals are linked to Gal/GalNAc and to GlcNac/NeuNAc. Similar to what it was observed in the Brunner's glands, in the HFD group a significant decrease of CTFC values in respect to the CTRL group binding takes place probably due to a decrease in glycosylation. Desulfation experiments did not increase significantly the binding intensity of SBA, PNA, WGA, and MAA-II, likely due to a lower number of sulfated residuals with respect to the CTRL group, confirming the results from HID stain. Lectin-binding to glycocalyx was not affected by the experimental treatment and presented residuals of Gal/GalNac, GlcNAc/NeuNAc, Glc/Man, and Fuc.

Our results indicate that HFD reduces the amount of glycosylated residuals, which parallels the downregulation of mucin synthesis observed in Kras-mutant mice induced by the same diet.[24] In both Kras and Double Knockout mutants, loss of O-glycans is associated with tumorigenesis[6,24] and our results suggest that wild type mice are also exposed to a higher risk of tumorigenesis when fed a HFD, due to the reduced synthesis of *Muc2*, which is regarded as an important tumor suppressor.[55] Like *Muc6*, galactosaminylation and fucosylation are reduced in HFD, and the consequences could be similar to those inferred for Brunner's glands.

In conclusion, our data demonstrate that in line with what it has been previously observed in the colon,

HFD affects both the amount and the glycosylation pattern of both *Muc2* and *Muc6*. Thus, a number of secreting cells in different tracts of the intestine are object of the alterations induced by the high-fat diet, increasing the risk of dysfunctions such as those related to gut microbiota and tumorigenesis.

Acknowledgments

The authors thank Patrizia Gena for technical help.

Competing Interests

The author(s) declared no potential conflicts of interest with respect to the research, authorship, and/or publication of this article.

Author Contributions

All authors have contributed to this article as follows: MM, GC, and GS conceived the study and wrote the article; GC designed and performed the experimental treatments; MM, DM, and GS performed the histological experiments and analyzed the data; all authors discussed the results, provided comments, and approved the manuscript as submitted.

Funding

The author(s) disclosed receipt of the following financial support for the research, authorship, and/or publication of this article: Financial support to GC and MM from Italian "Programmi di Ricerca Scientifica di Rilevante Interesse Nazionale 2017" (PRIN2017; grant # 2017J92TM5) is gratefully acknowledged.

ORCID iD

Maria Mastrodonato https://orcid.org/0000-0002-0799-8032

Literature Cited

1. Ouwerkerk JP, de Vos WM, Belzer C. Glycobiome: bacteria and mucus at the epithelial interface. Best Pract Res Clin Gastroenterol. 2013;27:25–38.
2. Linden SK, Sutton P, Karlsson NG, Korolik V, McGuckin MA. Mucins in the mucosal barrier to infection. Mucosal Immunol. 2008;1:183–97.
3. Johansson MEV, Ambort D, Pelaseyed T, Schütte A, Gustafsson JK, Ermund A, Subramani DB, Holmén-Larsson JM, Thomsson KA, Bergström JH, van der Post S, Rodriguez-Piñeiro AM, Sjövall H, Bäckström M, Hansson GC. Composition and functional role of the mucus layers in the intestine. Cell Mol Life Sci. 2011;68:3635–41.
4. Greening DW, Ji H, Kapp EA, Simpson RJ. Sulindac modulates secreted protein expression from LIM1215 colon carcinoma cells prior to apoptosis. Biochim Biophys Acta. 2013;1834:2293–307.
5. Di Luccia B, Mazzoli A, Cancelliere R, Crescenzo R, Ferrandino I, Monaco A, Bucci A, Naclerio G, Iossa S, Ricca E, Baccigalupi L. *Lactobacillus gasseri* SF1183 protects the intestinal epithelium and prevents colitis symptoms *in vivo*. J Funct Food. 2018;42:195–202.
6. Gao N, Bergstrom K, Fu J, Xie B, Chen W, Xia L. Loss of intestinal O-glycans promotes spontaneous duodenal tumors. Am J Physiol Gastrointest Liver Physiol. 2016;311:G74–83.
7. Moran AP, Gupta A, Joshi L. Sweet-talk: role of host glycosylation in bacterial pathogenesis of the gastrointestinal tract. Gut. 2011;60:1412–25.
8. Bergstrom KS, Xia L. Mucin-type O-glycans and their roles in intestinal homeostasis. Glycobiology. 2013;23:1026–37.
9. Kleessen B, Blaut M. Modulation of gut mucosal biofilms. Br J Nutr. 2005;93(Suppl. 1):S35–40.
10. Corfield AP, Myerscough N, Longman R, Sylvester P, Arul S, Pignatelli M. Mucins and mucosal protection in the gastrointestinal tract: new prospects for mucins in the pathology of gastrointestinal disease. Gut. 2000;47:589–94.
11. Sharpe C, Thornton DJ, Grencis RK. A sticky end for gastrointestinal helminths; the role of the mucus barrier. Parasite Immunol. 2018;40:e12517.
12. Pinho SS, Reis CA. Glycosylation in cancer: mechanisms and clinical implications. Nat Rev Cancer. 2015;15:540–55.
13. Vajaria BN, Patel PS. Glycosylation: a hallmark of cancer? Glycoconj J. 2017;34:147–56.
14. Nakamura N, Ota H, Katsuyama T, Akamatsu T, Ishihara K, Kurihara M, Hotta K. Histochemical reactivity of normal, metaplastic, and neoplastic tissues to alpha-linked N-acetylglucosamine residue-specific monoclonal antibody HIK1083. J Histochem Cytochem. 1998;46:793–801.
15. Shiroshita H, Watanabe H, Ajioka Y, Watanabe G, Nishikura K, Kitano S. Re-evaluation of mucin phenotypes of gastric minute well-differentiated-type adenocarcinomas using a series of HGM, MUC5AC, MUC6, M-GGMC, MUC2 and CD10 stains. Pathol Int. 2004;54:311–21.
16. Kavanaugh D, O'Callaghan J, Kilcoyne M, Kane M, Joshi L, Hickey RM. The intestinal glycome and its modulation by diet and nutrition. Nut Rev. 2015;73:359–75.
17. Buettner R, Scholmerich J, Bollheimer LC. High-fat diets: modeling the metabolic disorders of human obesity in rodents. Obesity (Silver Spring). 2007;15:798–808.
18. Winzell MS, Ahren B. The high-fat diet-fed mouse: a model for studying mechanisms and treatment of impaired glucose tolerance and type 2 diabetes. Diabetes. 2004;53(Suppl. 3):S215–9.
19. Calamita G, Portincasa P. Present and future therapeutic strategies in non-alcoholic fatty liver disease. Expert Opin Ther Targets. 2007;11:1231–49.
20. Singh RK, Chang HW, Yan D, Lee KM, Ucmak D, Wong K, Abrouk M, Farahnik B, Nakamura M, Zhu TH, Bhutani T, Liao W. Influence of diet on the gut

microbiome and implications for human health. J Transl Med. 2017;15:73.
21. Mastrodonato M, Mentino D, Portincasa P, Calamita G, Liquori GE, Ferri D. High-fat diet alters the oligosaccharide chains of colon mucins in mice. Histochem Cell Biol. 2014;142:449–59.
22. Jaswal VM, Babbar HS, Mann DS, Mahmood A. Maternal nutrition and development of intestinal functions: II—effect of feeding high protein and high fat diets to lactating rats. Indian J Exp Biol. 1990;28:776–9.
23. Gupta R, Jaswal VM, Mahmood A. Effect of high-fat diet on mice intestinal brush border membrane composition. Indian J Exp Biol. 1993;31:536–9.
24. Schulz MD, Atay C, Heringer J, Romrig FK, Schwitalla S, Aydin B, Ziegler PK, Varga J, Reindl W, Pommerenke C, Salinas-Riester G, Bock A, Alpert C, Blaut M, Polson SC, Brandl L, Kirchner T, Greten FR, Polson SW, Arkan MC. High-fat-diet-mediated dysbiosis promotes intestinal carcinogenesis independently of obesity. Nature. 2014;514:508–12.
25. Bartman AE, Buisine MP, Aubert JP, Niehans GA, Toribara NW, Kim YS, Kelly EJ, Crabtree JE, Ho SB. The MUC6 secretory mucin gene is expressed in a wide variety of epithelial tissues. J Pathol. 1998;186:398–405.
26. Krause WJ. Brunner's glands: a structural, histochemical and pathological profile. Prog Histochem Cytochem. 2000;35:255–367.
27. Schumacher U, Duku M, Katoh M, Jorns J, Krause WJ. Histochemical similarities of mucins produced by Brunner's glands and pyloric glands: a comparative study. Anat Rec A Discov Mol Cell Evol Biol. 2004;278:540–50.
28. Scillitani G, Mentino D. Comparative glycopattern analysis of mucins in the Brunner's glands of the guinea-pig and the house mouse (Rodentia). Acta Histochem. 2015;117:612–23.
29. Nakayama J. Dual roles of gastric gland mucin-specific O-glycans in prevention of gastric cancer. Acta Histochem Cytochem. 2014;47:1–9.
30. Kim K, Jang SJ, Song HJ, Yu E. Clinicopathologic characteristics and mucin expression in Brunner's gland proliferating lesions. Dig Dis Sci. 2013;58:194–201.
31. Accogli G, Crovace AM, Mastrodonato M, Rossi G, Francioso EG, Desantis S. Probiotic supplementation affects the glycan composition of mucins secreted by Brunner's glands of the pig duodenum. Ann Anat. 2018;218:236–42.
32. Scillitani G, Zizza S, Liquori GE, Ferri D. Histochemical and immunohistochemical evidence for a gradient in gastric juice production in the greater horseshoe bat, *Rhinolophus ferrumequinum* (Schreber, 1774). Acta Chiropterol. 2005;7:301–8.
33. Mastrodonato M, Calamita G, Rossi R, Scillitani G, Liquori GE, Ferri D. Expression of H(+), K(+)-ATPase and glycopattern analysis in the gastric glands of Rana esculenta. J Histochem Cytochem. 2009;57:215–25.
34. Petraccioli A, Maio N, Guarino FM, Scillitani G. Seasonal variation in glycoconjugates of the pedal glandular system of the rayed Mediterranean limpet, *Patella caerulea* (Gastropoda: Patellidae). Zoology (Jena). 2013;116:186–96.
35. Scillitani G, Moramarco AM, Rossi R, Mastrodonato M. Glycopattern analysis and structure of the egg extracellular matrix in the Apennine yellow-bellied toad, Bombina pachypus (Anura: Bombinatoridae). Folia Histochem Cytobiol. 2011;49:306–16.
36. Liquori GE, Mastrodonato M, Mentino D, Scillitani G, Desantis S, Portincasa P, Ferri D. In situ characterization of O-linked glycans of Muc2 in mouse colon. Acta Histochem. 2012;114:723–32.
37. Mentino D, Mastrodonato M, Rossi R, Scillitani G. Histochemical and structural characterization of egg extra-cellular matrix in bufonid toads, *Bufo bufo* and *Bufotes balearicus*: molecular diversity versus morphological uniformity. Microsc Res Tech. 2014;77:910–7.
38. Katsuyama T, Spicer SS. Histochemical differentiation of complex carbohydrates with variants of the concanavalin A-horseradish peroxidase method. J Histochem Cytochem. 1978;26:233–50.
39. Liquori GE, Zizza S, Mastrodonato M, Scillitani G, Calamita G, Ferri D. Pepsinogen and H, K-ATPase mediate acid secretion in gastric glands of Triturus carnifex (Amphibia, Caudata). Acta Histochem. 2005;107:133–41.
40. Ruifrok AC, Johnston DA. Quantification of histochemical staining by color deconvolution. Anal Quant Cytol Histol. 2001;23:291–9.
41. Landini G. Novel context-based segmentation algorithms for intelligent microscopy. Birmingham Blogs: University of Birmingham; 2019. Available from: https://blog.bham.ac.uk/intellimic/g-landini-software/colour-deconvolution/
42. Mastrodonato M, Mentino D, Lopedota A, Cutrignelli A, Scillitani G. A histochemical approach to glycan diversity in the urothelium of pig urinary bladder. Microsc Res Tech. 2017;80:239–49.
43. Rasband W. ImageJ. Bethesda, MD: National Institutes of Health (US); 2018. Available from: http://imagej.nih.gov/ij/
44. McCloy RA, Rogers S, Caldon CE, Lorca T, Castro A, Burgess A. Partial inhibition of Cdk1 in G_2 phase overrides the SAC and decouples mitotic events. Cell Cycle. 2014;13:1400–12.
45. Gay F, Ferrandino I, Monaco A, Cerulo M, Capasso G, Capaldo A. Histological and hormonal changes in the European eel (Anguilla anguilla) after exposure to environmental cocaine concentration. J Fish Dis. 2016;39:295–308.
46. Zaiontz C. Real statistical analysis using excel. Release 6.8; 2019. Available from: www.real-statistics.com
47. Ermund A, Schutte A, Johansson ME, Gustafsson JK, Hansson GC. Studies of mucus in mouse stomach, small intestine, and colon. I. Gastrointestinal mucus layers have different properties depending on location as well as over the Peyer's patches. Am J Physiol Gastrointest Liver Physiol. 2013;305:G341–7.

48. Liquori GE, Calamita G, Cascella D, Mastrodonato M, Portincasa P, Ferri D. An innovative methodology for the automated morphometric and quantitative estimation of liver steatosis. Histol Histopathol. 2009;24:49–60.
49. Moore BA, Morris GP, Vanner S. A novel in vitro model of Brunner's gland secretion in the guinea pig duodenum. Am J Physiol-gastr L. 2000;278:G477–85.
50. Ishihara K, Kurihara M, Goso Y, Urata T, Ota H, Katsuyama T, Hotta K. Peripheral alpha-linked N-acetylglucosamine on the carbohydrate moiety of mucin derived from mammalian gastric gland mucous cells: epitope recognized by a newly characterized monoclonal antibody. Biochem J. 1996;318:409–16.
51. Saha A, Gaurav AK, Bhattacharya S, Bhattacharya A. Molecular basis of pathogenesis in amoebiasis. Curr Clin Microbiol Rep. 2015;2:143–54.
52. Becker DJ, Lowe JB. Fucose: biosynthesis and biological function in mammals. Glycobiology. 2003;13:41R–53R.
53. Moriwaki K, Miyoshi E. Fucosylation and gastrointestinal cancer. World J Hepatol. 2010;2:151–61.
54. Kawashima H. Roles of sulfated glycans in lymphocyte homing. Biol Pharm Bull. 2006;29:2343–9.
55. Velcich A, Yang W, Heyer J, Fragale A, Nicholas C, Viani S, Kucherlapati R, Lipkin M, Yang K, Augenlicht L. Colorectal cancer in mice genetically deficient in the mucin Muc2. Science. 2002;295:1726–9.